Wave Propagation in a LRPC Composite Double Panel Structure with Periodically Attached Pillars and Etched Holes

Denghui QIAN

Jiangsu Province Key Laboratory of Structure Engineering
College of Civil Engineering
Suzhou University of Science and Technology
Suzhou 215011, Jiangsu, China; e-mail: dhqian@usts.edu.cn

The locally resonant phononic crystal (LRPC) composite double panel structure (DPS) made of a two-dimensional periodic array of a two-component cylindrical LR pillar connected between the upper and lower composite plates is proposed. The plates are composed of two kinds of materials and periodically etched holes. In order to reveal the bandgap properties of structure theoretically, the band structures, displacement fields of eigenmodes and transmission power spectrums of corresponding 8×8 finite structure are calculated and displayed by using finite element method (FEM). Numerical results and further analysis demonstrate that if the excitation and response points are picked on different sides of the structure, a wide band gap with low starting frequency is opened, which can be treated as the coupling between dominant vibrations of pillars and plate modes. In addition, the influences of filled-in rubber, etched hole and viscidity of soft material on band gap are studied and understood with the help of "base-spring-mass" simplified model.

Keywords: locally resonant phononic crystal; composite double panel structure; band structure; displacement field; transmission power spectrum; "base-spring-mass" simplified model.

1. Introduction

With the improvement of industry level, the requirement for comfort is increasing with each passing day. In many areas of engineering, different kinds of plates are extensively applied as the containment structures (PIETRZKO, MAO, 2008; CARNEAL, FULLER, 2004). Particularly, DPSs are more popular than single plates on account of the multi-function properties such as excellent shock resistance, light-quality, large-stiffness, good thermal diffusivity and so on (QIAN, SHI, 2016). Researches have indicated that containment structure is the main propagation medium of vibration, which is also the source for radiating noise (QIAN, SHI, 2016; BENJEDDOU, 2001). Thus, the researches on vibration propagation in DPS will play an important role in restraining the structure vibration and reducing the radiated noise.

In recent years, the periodic composite structure named as PC has attracted a lot of attention (SIGALAS, ECONOMOU, 1992; MARTÍNEZ-SALA *et al.*, 1995; LIU *et al.*, 2000), which provides a new idea for controlling the vibration and noise propagating along the containment structure. Studies on formation mechanisms of band gap have revealed two kinds: Bragg scattering (SIGALAS, ECONOMOU, 1992; MARTÍNEZ-SALA *et al.*, 1995; KUSHWAHA *et al.*, 1994; JAMES *et al.*, 1995) and locally resonant (LR) (LIU *et al.*, 2000; WANG *et al.*, 2004; SAINIDOU *et al.*, 2006). The main difference between them is that the frequency range of band gap formed by LR is almost two orders of magnitude lower than that formed by Bragg scattering (LIU *et al.*, 2000), which illustrates that the PCs designed based on the second mechanism can be applied to control the vibration and noise in low frequency region. Hence, introducing the design idea of LRPC to different kinds of DPSs and researching the displayed bandgap properties will provide a new idea to restrain the structure vibration and reduce the noise in the unmanageable low frequency region (OUDICH *et al.*, 2011; XIAO *et al.*, 2012) of some industrial products.

Recently, researches on plates with the design idea of LRPC introduced have appeared. Two main types of structures have formed: the filled-in structure is

constructed by periodically etching holes in a base plate and then filling them with soft scatters; and the stubbed-on structure is constructed by periodically attaching resonant units onto the surface of base plate (MA *et al.*, 2014; QIAN, SHI, 2017a). The vibration band gaps of epoxy base plates with filled-in rubber resonant units and filled-in rubber-coated heavy mass resonant units were investigated by HSU and WU (2007) and XIAO *et al.* (2008), which can be regarded as the two-component and three-component filled-in structures. Similarly, OUDICH *et al.* (2010) researched the two-component and three-component stubbed-on structures constructed by periodically attaching rubber stubs without and with Pb capped on the surface of base plate. Combining the two types, the propagation characteristics of Lamb waves in a LRPC composite plate with the combined resonant unit were studied by LI *et al.* (2015). As the simplify of filled-in and stubbed-on structures, the propagation characteristics of flexural waves in the simplified model of composite LRPC single plate were investigated by QIAN and SHI (2017b).

In this paper, we investigate the propagation characteristics of flexural and longitudinal vibrations in a LRPC composite DPS consisting of a two-layer composite plate with periodically attached cylindrical LR pillars in the cavity and etched holes in the upper and lower plates. At first, the band structures, displacement fields of eigenmodes and transmission power spectrums of the corresponding finite structure are calculated by FEM to study the formation mechanisms of band gap. Then in order to reveal the influences of filled-in scatters and etched holes on band structure, two groups of contrast are constructed. Further, the influences of filled-in rubber radius, etched hole radius and viscidity of soft material on band gap are discussed. All the results are expected to be of theoretic significances and engineering application prospects in the field of vibration and noise control.

2. Model and method

As shown schematically in Fig. 1a, the studied physical model is constructed by periodically depositing the two-component cylindrical LR pillars squarely onto the surfaces of the upper and lower two-dimensional binary LRPC plates, which consist of an array of rubber inclusions embedded in epoxy matrix with a finite thickness. In a unit cell, the material of first and last layers in the pillar is rubber, and the materials of plates and middle layer in the pillar are epoxy and Pb, respectively. The lattice constant, the thickness of base plate, the radius of pillar, the radius of filled-in rubber in the base plate, and the heights of different layers in the pillar are denoted by a, e, r, R, h_1 and h_2, respectively. Besides, another model with both periodically attached pillars and etched holes is
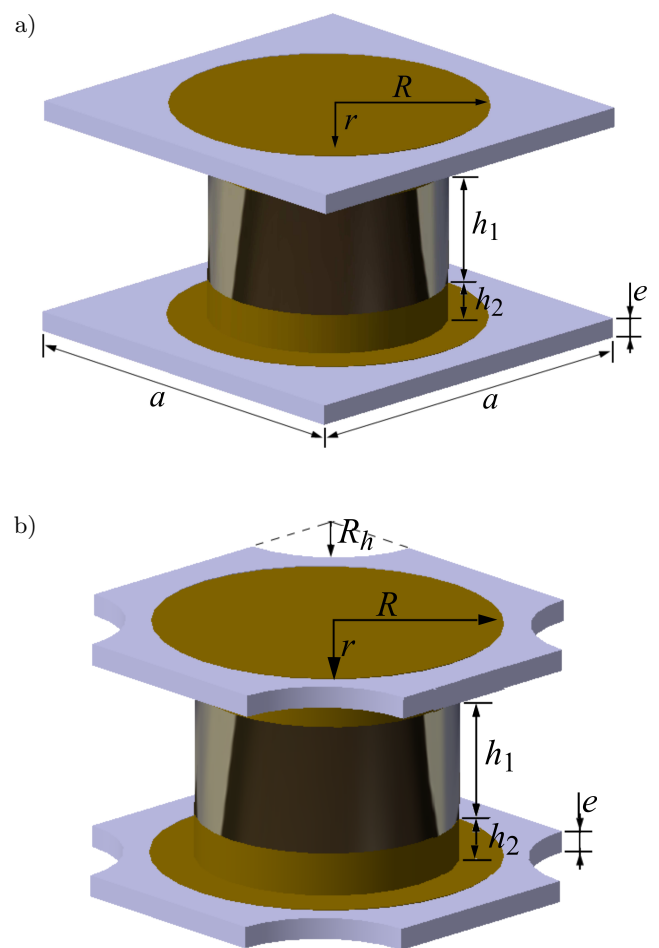

Fig. 1. The unit cells of LRPC composite DPSs (a) without and (b) with periodically etched holes.

proposed as shown in Fig. 1b. The radius of hole is R_h. Table 1 displays the materials' parameters used in the calculations, and all materials are assumed to be elastically isotropic.

Table 1. Materials' parameters used in calculations.

Material	Mass density [kg/m³]	Young's modulus [10^{10} N/m²]	Poission's ratio
Epoxy	1180	0.435	0.368
Rubber	1300	$1.175 \cdot 10^{-5}$	0.469
Pb	11 600	4.08	0.370

Band structures of the proposed models are calculated by the finite element method (FEM), which is implemented by adopting the commercial software, COMSOL Multiphysics. For the mesh elements, the default tetrahedral mesh provided by the software is used. In the calculation, only one unit cell is taken into consideration, which can be attributed to the periodicity of the structure. The stress-free boundary condi-

tions are applied to the free surfaces, and the periodic boundary conditions according to Bloch-Floquet theorem are used for the interfaces between the nearest unit cells (QIAN, SHI, 2017a; XIAO et al., 2008; OUDICH et al., 2010)

$$u_i(x+a, y+a) = u_i(x,y)e^{-i(k_x a + k_y a)}, \quad (i = x, y, z), \quad (1)$$

where u_i represents the elastic displacement $\mathbf{u}$ along x-direction, y-direction and z-direction respectively when i equals to x, y and z; k_x and k_y are the components of Bloch wave vector $\mathbf{k}$ limited in the irreducible first Brillouin zone (1BZ).

Substituting Eq. (1) to characteristic equation of FEM gives:

$$(\mathbf{K} - \omega^2 \mathbf{M})\mathbf{u} = \mathbf{0}. \quad (2)$$

Particularly noted, the elements in stiffness matrix $\mathbf{K}$ and mass matrix $\mathbf{M}$ are coupled with the items containing the Bloch wave vector, which are not the original structural stiffness and mass matrices any more.

Equation (2) represents a generalized eigenvalue problem for ω^2. Finally, the band structure can be obtained by solving the equation for each Bloch wave vector limited in the irreducible first Brillouin zone (1BZ).

3. Numerical results and analyses

3.1. Band structure of LRPC composite DPS without etched holes

Figure 2b shows the band structure of LRPC composite DPS with the holes not etched. All the materials' parameters and geometric parameters used in the calculation are shown in Tables 1 and 2, respectively. To verify the accuracy of the calculated result, the transmission power spectrums of flexural and longitudinal vibrations in the corresponding finite structure are displayed in Fig. 2a and 2c, separately. In this work, the finite DPS is made of 8×8 unit cells and the excitation point is picked on one end of the lower plate as well as the response point is picked on the other end of the upper plate, as shown in Fig. 3.

Table 2. Geometric parameters used in calculations.

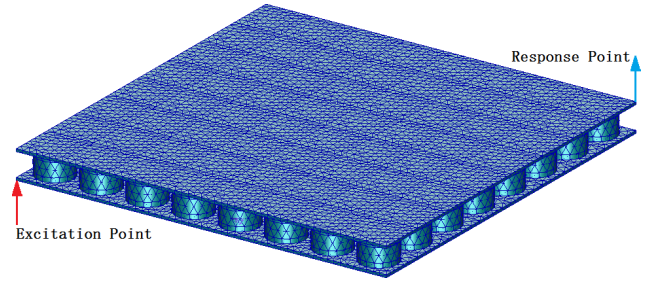| a [m]	e [m]	r [m]	R [m]	R_h [m]	h_1 [m]	h_2 [m]
0.1	0.005	0.04	0.04	0.02	0.01	0.03

Fig. 3. Meshing of the finite LRPC DPS made of 8×8 unit cells (QIAN, SHI, 2017a).

As shown in Fig. 2b, a narrow complete band gap is opened between 31 Hz and 75 Hz. But from Fig. 2a and 2c, the frequency range of attenuation in the transmission power spectrum is very wide no matter the finite structure is vibrated flexural or longitudinal,
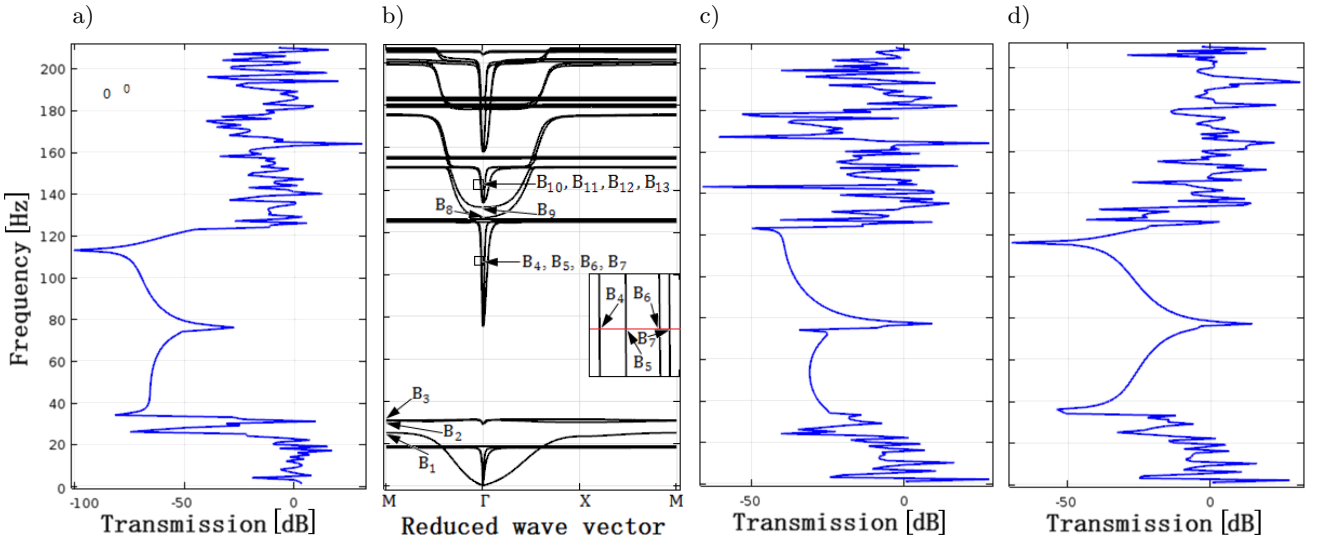

Fig. 2. Band structure of LRPC composite DPS and transmission power spectrums of the corresponding finite 8×8 structure: a) transmission power spectrum of flexural vibration when the excitation and response points are picked on different plates; b) band structure; c) transmission power spectrum of longitudinal vibration when the excitation and response points are picked on different plates; d) transmission power spectrum of longitudinal vibration when both the excitation and response points are picked on same plate.

which should have matched well with the frequency range of the band gap (QIAN, SHI, 2016; XIAO *et al.*, 2012). To find more attenuation characteristics, both the excitation and response points are picked on the lower plate and the transmission power spectrum of longitudinal vibration is shown in Fig. 2d. From it, hardly any frequency range of attenuation can be observed. To reveal the mechanisms of the typical phenomena displayed in transmission power spectrums of the LRPC composite DPS, the displacement fields of eigenmodes labeled in Fig. 2b are shown in Fig. 4.

For modes B_1, B_8 and B_9, the dominant vibration translating along z-direction couples with the out-of-plane plate mode of upper and lower plates. In mode B_1, the vibration energy is concentrated in the pillar with the two plates static. Both in modes B_8 and B_9, the middle Pb layer of pillar acts as the stationary

layer. What's opposite, the two base plates achieve dynamic balance in the inverse flexural vibration in mode B_8 while the uniform flexural vibration of the two plates achieve dynamic balance in mode B_9, based on which, modes B_8 and B_9 are called as the symmetric and antisymmetric flexural vibration modes, respectively. As a result of the coupling, a partial flexural vibration band gap between B_1 and B_8 with frequency interval 25–126 Hz is opened, which is why the big attenuation exists in the transmission power spectrum of the flexural vibration, as shown in Fig. 2a.

For modes B_2 and B_3, the dominant vibration rotating in xy plane couples with the out-of-plane shear deformation of upper and lower plates. Both modes B_2 and B_3 concentrate the vibration energy in the pillar with the two plates stationary. As for modes B_4–B_7, they can be treated as the result of the coupling between the dominant vibration translating in xy
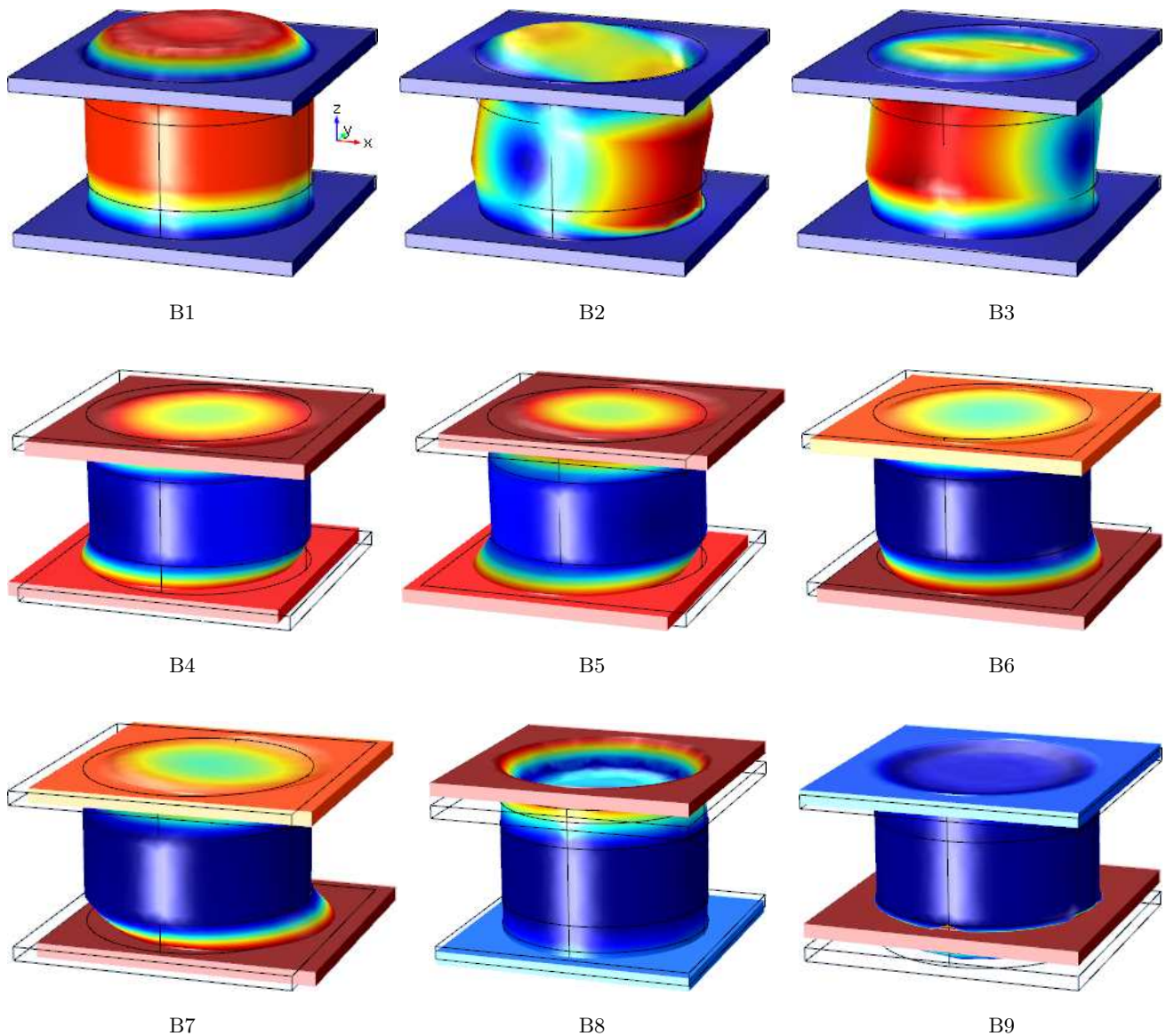

Fig. 4. The displacement fields of eigenmodes labeled in Fig. 2b.

plane and the in-plane shear deformation of upper and lower plates. In all the four modes, the middle Pb layer of pillar keeps stationary. Meanwhile, the uniform longitudinal vibration of lower and upper plates achieve dynamic balance in mode B_4 and B_5 while the two plates achieve dynamic balance in the inverse longitudinal vibration in mode B_6 and B_7. Similarly, modes B_4–B_5 and modes B_6–B_7 are called as the antisymmetric longitudinal vibration mode and symmetric longitudinal vibration mode. As a result of the couplings, a partial longitudinal vibration band gap with frequency interval 31–75 Hz is opened. The corresponding attenuations existed in the transmission power spectrums of the longitudinal vibration shown in Fig. 2c and 2d are not obvious, which has been explained in (OUDICH et al., 2010).

What should be noted is that, the vibration of upper plate is weakened because the vibration phases of upper plate in the antisymmetric longitudinal vibration mode B_4 and symmetric longitudinal vibration mode B_6 are inverse, as well as in B_5 and B_7. Based on this, the big attenuation displayed in the transmission spectrum of longitudinal vibration shown in Fig. 2c can be understood. Meanwhile, the attenuation is absent in Fig. 2d because the lower plate is vibrated strongly with the uniform phase. The details can be referred to (QIAN, SHI, 2017a).

Moreover, as shown in Fig. 5, the "base-spring-mass" simplified model is applied to help understand the influence rules, which has been investigated semi-analytically in detail (WANG et al., 2011; WANG, WANG, 2013). For modes B_1–B_3, the epoxy layer, rubber layer and Pb layer can be treated as the base, equivalent spring and mass respectively; and for modes $B_4$$B_9$, the Pb layer, rubber layer and epoxy layer can be treated as the base, equivalent spring and mass separately. Besides, the equivalent spring and mass of each mode can be calculated approximatively (WANG et al., 2011).
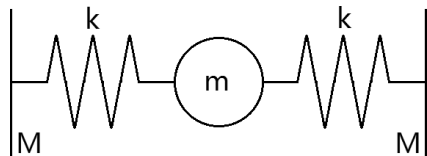

Fig. 5. The "base-spring-mass" simplified model applied to help understand the vibration modes.

In (QIAN, SHI, 2017a), the LRPC DPS with the base plates consisted of only one material is studied. The band structure with the same parameters in this paper is shown in Fig. 6. By comparing Fig. 2b with Fig. 6, all the bands are moved down to the lower frequency region and the band structure is divided to layered distribution in the effect of filled-in rubber. With the help of "base-spring-mass" simplified model, the
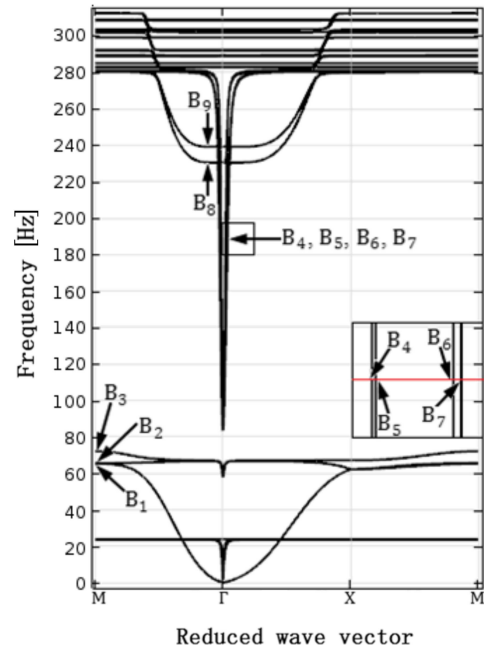

Fig. 6. Band structure of LRPC DPS with the base plates consisted of only one material (QIAN, SHI, 2017a).

filled-in and stubbed-on rubbers can be regarded as the series connection of two equivalent springs, which results in the reduce of original spring stiffness. In addition, the complete bandgap width opened between B_3 and B_4 is wider in Fig. 2b than Fig. 6, which can be attributed to that the effect of filled-in rubber on B_1–B_3 is larger than B_4–B_7. If the excitation and response points are on different sides of DPS, the bandgap width is reduced from 158 Hz (72–230 Hz) to 95 Hz (31–126 Hz) and the starting frequency is decreased from 72 Hz to 31 Hz, which illustrates that filling rubber in plate makes it possible to control lower sound and vibration, but which narrows the bandgap width.

3.2. Band structure of LRPC composite DPS with periodically etched holes

Figure 7 shows the band structure of LRPC composite DPS with periodically etched holes. All the materials' parameters and geometric parameters used in the calculation are same as the example in Fig. 2b, as shown in Tables 1 and 2, respectively.

By comparing Fig. 7 and Fig. 2b, the etched holes have obvious effects on modes B_4–B_9, but little effects on B_1–B_3, which can be explained by applying the "base-spring-mass" simplified model. For B_1–B_3, because the plates are equivalent to the static base, holes have nothing to do with the modes; but for B_4–B_9, the corresponding frequencies of bands increase because the plates are equivalent to mass and the etched holes make the equivalent mass decrease. Eventually, etching holes in the upper and lower base plates can
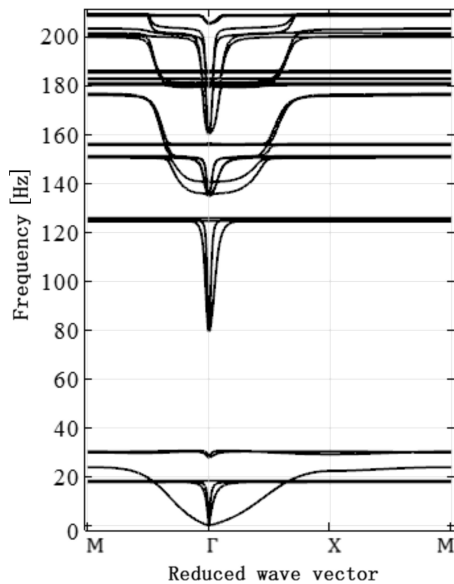
Fig. 7. Band structure of LRPC composite DPS with periodically etched holes.

not only widen the bandgap, but keep the starting frequency unchanged.

3.3. Influences of parameters on band gap

The influences of base plates and stubbed-on pillar on band gap have been investigated in detail in (QIAN, SHI, 2017a). Here, the effects of filled-in rubber and etched hole on band gap are studied. During the study, the radius of rubber R and radius of hole R_h are chosen as the influencing parameters. Besides, the rest parameters are same as the ones of the example shown in Fig. 2a while considering the influences of one parameter on the starting frequency f_1 (or f_3), cutoff frequency f_8 and bandgap width f_w.

Figure 8 shows the influences of filled-in rubber radius R on f_1, f_3, f_8 and f_w. In the figure, all of
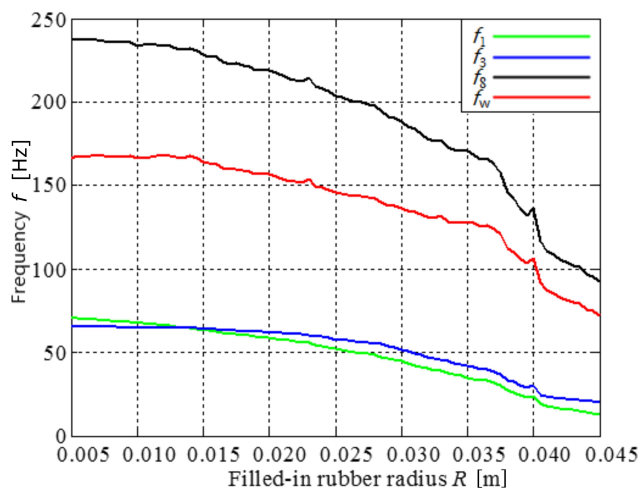

Fig. 8. The influences of filled-in rubber radius R on f_1, f_3, f_8 and f_w.

f_1, f_3 and f_8 decrease with the increase of R, which can be understood by the "base-spring-mass" simplified model. In the model, the filled-in rubber is simplified as the spring and the equivalent stiffness decreases with the increase of R. In addition, bandgap width f_w is decided by the starting frequency f_3 and ending frequency f_8 if $R < 0.014$ m; but f_w is decided by the starting frequency f_1 and ending frequency f_8 if $R \geq 0.014$ m. As shown in the figure, f_w also decreases with the increase of R, which illustrates that the effects of filled-in rubber on mode B_8 is bigger than modes B_1 and B_3. In general, increasing the rubber radius can play an active role in lowering the starting frequency, but narrowing the bandgap width.

Figure 9 shows the influences of etched hole radius R_h on f_1, f_3, f_8 and f_w. In the figure, R_h has no effects on f_1 and f_3, which can be attributed to that in "base-spring-mass" simplified model, the plates can be equivalent to base in modes B_1 and B_3. But f_8 increases with the increase of R_h, which is because in the model, the plates are equivalent to mass in modes B_8 and the equivalent mass decreases with the increase of R_h. Hence, the increase of f_8 and constant of f_3 lead f_w to increase with the increase of R_h. In general, increasing the radius of etched hole can not only play as active role in widening the bandgap, but also keeping the starting frequency unchanged.
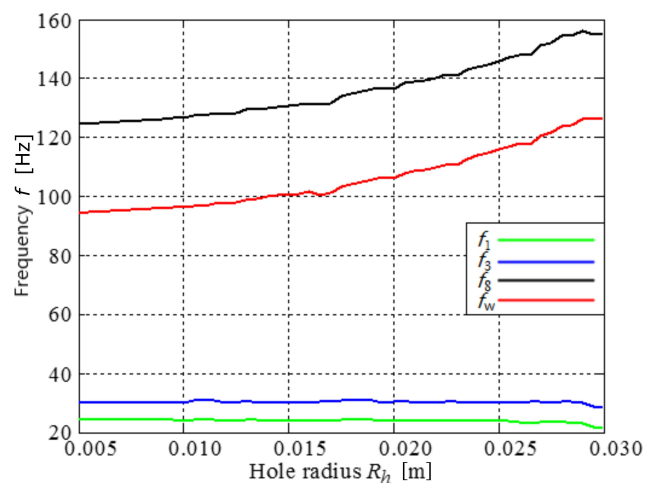

Fig. 9. The influences of etched hole radius R_h on f_1, f_3, f_8 and f_w.

If the viscidity of soft material is considered, the elasticity moduli and shear modulus are relevant to the frequency in frequency domain. Hence, the eigenvalue problem of Eq. (2) should be solved by iterative process, and the detailed calculation steps are described in (QIAN, SHI, 2017b; ZHAO, WEI, 2009; WEI, ZHAO, 2010; ZHU et al., 2016).

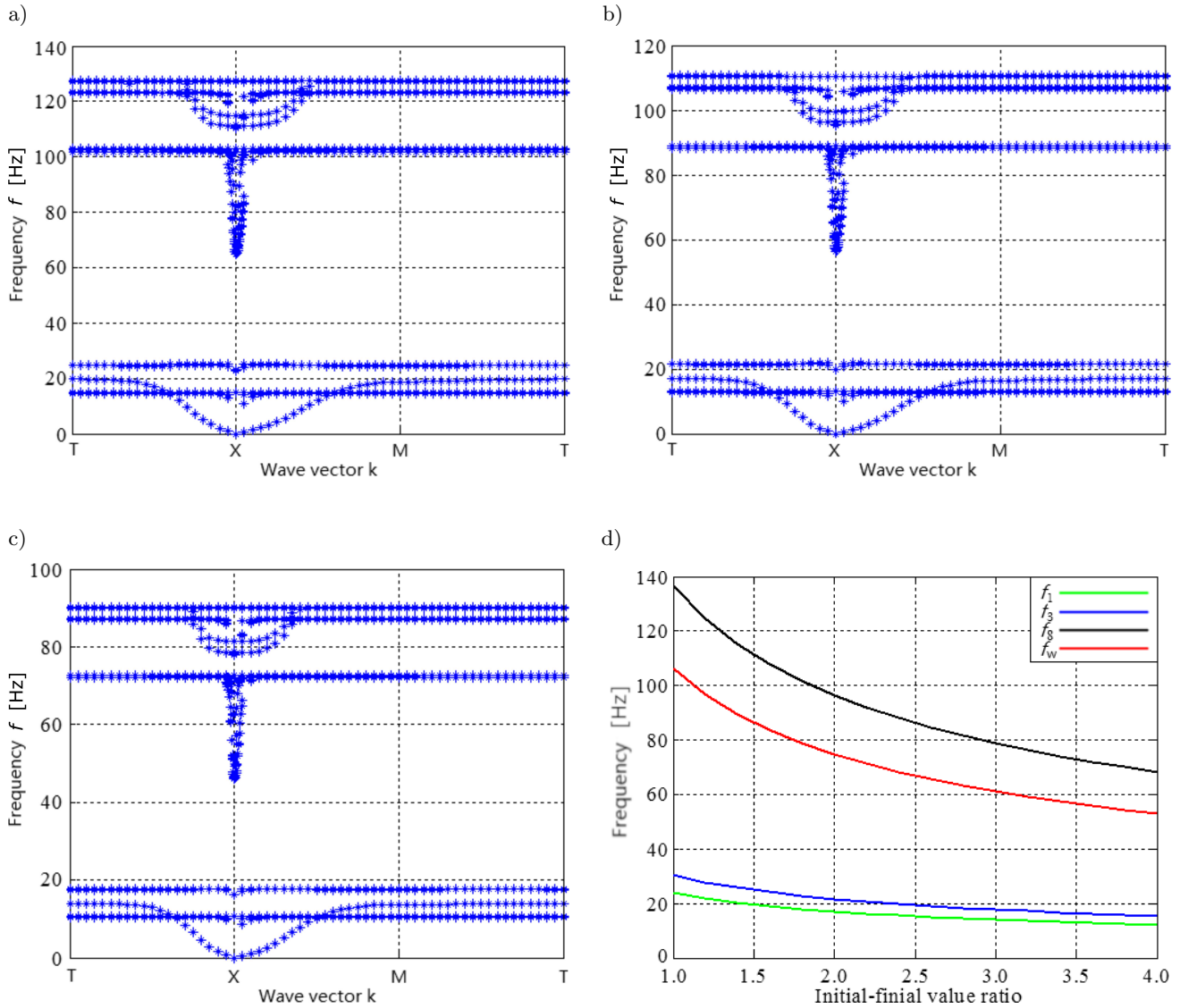Figures 10a, b and c display the band structures of hole-etched LRPC composite DPS with the

a)

b)

c)

d)

Fig. 10. Band structures of hole-etched LRPC composite DPS with the viscidity of soft material considered when relax time $\tau = 3 \cdot 10^{-5}$ s, initial-final value ratio: a) $\alpha = 1.5$, b) $\alpha = 2.0$, c) $\alpha = 3.0$, and d) the influences of initial-final value ratio α on critical frequencies f_1, f_3, f_8 and bandgap width f_w.

viscidity of soft material considered when relax time $\tau = 3 \cdot 10^{-5}$ s, initial-final value ratio $\alpha = 1.5$, 2.0 and 3.0, respectively. Here, all the parameters used in the calculation are shown in Tables 1 and 2. As shown in the figure, all the bands are affected by α obviously. In order to further illustrate the influence rule, the influences of α on critical frequencies f_1, f_3, f_8 and bandgap width f_w are displayed in Fig. 10d. As sketched in the figure, all of the frequencies f_1, f_3 and f_8 decrease with the increase of α and the slope of ending frequency f_8 is larger than that of starting frequency f_3, which lead the bandgap width to decrease with the increase of α. In consequence, increasing the initial-final value ratio of soft material plays a role in lowering the starting frequency, but narrowing the bandgap width.

Figures 11a, b and c display the band structures of hole-etched LRPC composite DPS with the viscidity of soft material considered when initial-final value ratio $\alpha = 2.0$, relax time $\tau = 3 \cdot 10^{-5}$ s, $1 \cdot 10^{-4}$ s and $5 \cdot 10^{-4}$ s, respectively. Here, all the parameters used in the calculation are shown in Tables 1 and 2. As shown in the figure, the bands in high frequency range are affected by τ obviously. The influences of τ on critical frequencies f_1, f_3, f_8 and bandgap width f_w are also displayed in Fig. 11d. With the increase of τ, f_8 increases, but f_1, f_3 keep constant. Hence, the increase of f_8 and constant of f_3 lead f_w to increase with the increase of τ. In general, increasing the relax time of soft material can not only play an active role in widening the bandgap, but also keeping the starting frequency unchanged.
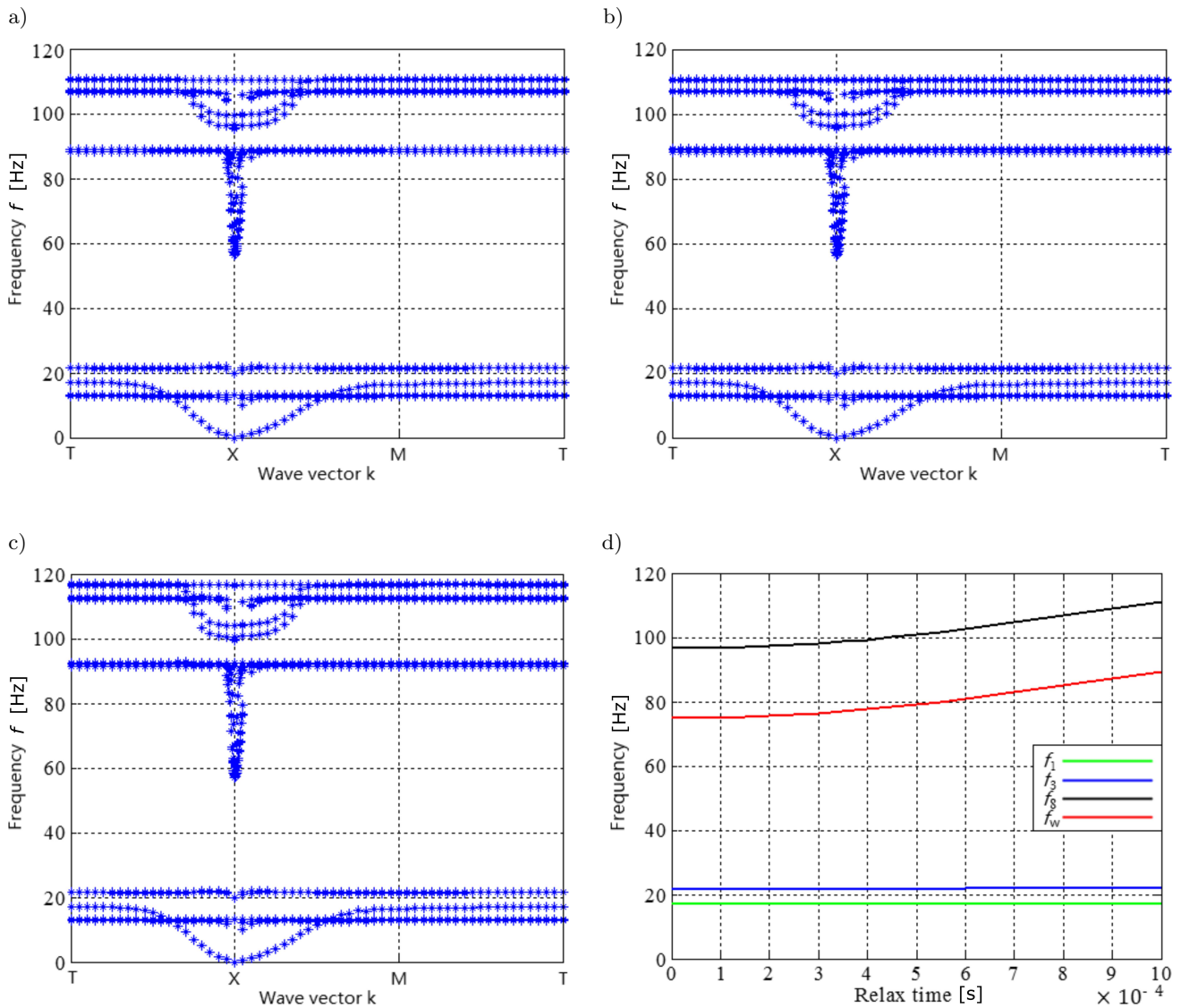
Fig. 11. Band structures of hole-etched LRPC composite DPS with the viscidity of soft material considered when initial-final value ratio $\alpha = 2.0$, relax time (a) $\tau = 3 \cdot 10^{-5}$ s, b) $\tau = 1 \cdot 10^{-4}$ s, c) $\tau = 5 \cdot 10^{-4}$ s, and d) the influences of relax time τ on critical frequencies f_1, f_3, f_8 and bandgap width f_w.

4. Conclusions

In this paper, the LRPC composite DPS with periodically attached pillars and etched holes is proposed and the bandgap properties of structure are investigated by applying FEM. The main conclusions are as follows:

1) A complete band gap with low starting frequency and wide bandgap width is opened according to the analysis of band structure and transmission power spectrums when the excitation and response points are on different sides of structure, and the formation mechanisms of band gap are revealed with the help of displacement fields of eigenmodes.

2) By comparing the band structures of LRPC composite DPSs with and without filled-in rubber, the rubber can lower the starting frequency, but narrow the bandgap width at the same time. By etching holes in the plates, it can not only widen the bandgap, but keep the starting frequency unchanged. Besides, both the starting frequency and bandgap width decreases with the increase of rubber radius. But the bandgap width increases and the starting frequency keeps still with the increase of etched hole radius.

3) If the viscidity of soft material is considered, increasing the initial-final value ratio of soft material plays a role in lowering the starting frequency, but narrowing the bandgap width. But increasing the relax time of soft material can not only play an active role in widening the bandgap, but also keeping the starting frequency unchanged.

Acknowledgments

References

1. BENJEDDOU A. (2001), *Advances in hybrid active-passive vibration and noise control via piezoelectric and viscoelastic constrained layer treatments*, Journal of Vibration and Control, **7**, 4, 565–602.

2. CARNEAL J.P., FULLER C.R. (2004), *An analytical and experimental investigation of active structural acoustic control of noise transmission through double panel systems*, Journal of Sound and Vibration, **272**, 3–5, 749-771.

3. HSU J.C., WU T.T. (2007), *Lamb waves in binary locally resonant phononic plates with two-dimensional lattices*, Applied Physics Letters, **90**, 20, 201904–201907.

4. JAMES R., WOODLEY S.M., DYER C.M., HUMPHREY V.F. (1995), *Sonic bands, bandgaps, and defect states in layered structures – theory and experiment*, Journal of the Acoustical Society of America, **97**, 4, 2041–2047.

5. KUSHWAHA M.S., HALEVI P., MARTÍNEZ G., DOBRZYŃSKI L., DJAFARI-ROUHANI B. (1994), *Theory of acoustic band structure of periodic elastic composites*, Physical Review B: Condensed Matter, **49**, 4, 2313–2322.

6. LI Y., CHEN T., WANG X., XI Y., LIANG Q. (2015), *Enlargement of locally resonant sonic band gap by using composite plate-type acoustic metamaterial*, Physics Letters A, **379**, 5, 412–416.

7. LIU Z. et al. (2000), *Locally resonant sonic materials*, Science, **289**, 5485, 1734–1736.

8. MA J., HOU Z., ASSOUAR B.M. (2014), *Opening a large full phononic band gap in thin elastic plate with resonant units*, Journal of Applied Physics, **115**, 9, 093508–093513.

9. MARTÍNEZ-SALA R., SANCHO J., SÁNCHEZ J.V., GÓMEZ V., LLINARES J. (1995), *Sound attenuation by sculpture*, Nature, **378**, 6554, 241–241.

10. OUDICH M., LI Y., ASSOUAR B.M., HOU Z. (2010), *A sonic band gap based on the locally resonant phononic plates with stubs*, New Journal of Physics, **12**, 2, 201–206.

11. OUDICH M. et al. (2011), *Experimental evidence of locally resonant sonic band gap in two-dimensional phononic stubbed plates*, Physical Review B, **84**, 16, 667–673.

12. PIETRZKO S.J., MAO Q. (2008), *New results in active and passive control of sound transmission through double wall structures*, Aerospace Science and Technology, **12**, 1, 42–53.

13. QIAN D., SHI Z. (2016), *Bandgap properties in locally resonant phononic crystal double panel structures with periodically attached spring-mass resonators*, Physics Letters A, **380**, 41, 3319–3325.

14. QIAN D., SHI Z. (2017a), *Bandgap properties in locally resonant phononic crystal double panel structures with periodically attached pillars*, Journal of Theoretical and Applied Mechanics, **55**, 4, 1167–1179.

15. QIAN D., SHI Z. (2017b), *Bandgap properties in simplified model of composite locally resonant phononic crystal plate*, Physics Letters A, **381**, 40, 3505–3513.

16. SAINIDOU R., DJAFARI-ROUHANI B., PENNEC Y., VASSEUR J.O. (2006), *Locally resonant phononic crystals made of hollow spheres or cylinders*, Physical Review B, **73**, 2, 024302.

17. SIGALAS M.M., ECONOMOU E.N. (1992), *Elastic and acoustic wave band structure*, Journal of Sound and Vibration, **158**, 2, 377–382.

18. WANG G., WEN X., WEN J., SHAO L., LIU Y. (2004), *Two-dimensional locally resonant phononic crystals with binary structures*, Physical Review Letters, **93**, 15, 154302.

19. WANG Y.F., WANG Y.S. (2013), *Complete bandgaps in two-dimensional phononic crystal slabs with resonators*, Journal of Applied Physics, **114**, 4, 2022.

20. WANG Y.F., WANG Y.S., SU X.X. (2011), *Large bandgaps of two-dimensional phononic crystals with cross-like holes*, Journal of Applied Physics, **110**, 11, 2059.

21. WEI P.J., ZHAO Y.P. (2010), *The influence of viscosity on band gaps of 2D phononic crystal*, Mechanics of Advanced Materials and Structures, **17**, 6, 383–392.

22. XIAO W., ZENG G.W., CHENG Y.S. (2008), *Flexural vibration band gaps in a thin plate containing a periodic array of hemmed discs*, Applied Acoustics, **69**, 3, 255–261.

23. XIAO Y., WEN J., WEN X. (2012), *Flexural wave band gaps in locally resonant thin plates with periodically attached spring-mass resonators*, Journal of Physics D: Applied Physics, **45**, 19, 195401–195412.

24. ZHAO Y.P., WEI P.J. (2009), *The band gap of 1D viscoelastic phononic crystal*, Computational Materials Science, **46**, 3, 603–606.

25. ZHU X., ZHONG S., ZHAO H. (2016), *Band gap structures for viscoelastic phononic crystals based on numerical and experimental investigation*, Applied Acoustics, **106**, 93–104.